New Generation Computing
https://doi.org/10.1007/s00354-022-00183-1

Forecasting COVID19 Reliability of the Countries by Using Non-Homogeneous Poisson Process Models

Nevin Guler Dincer[1] · Serdar Demir[1] · Muhammet Oğuzhan Yalçin[1]

Received: 3 January 2022 / Accepted: 9 June 2022

Abstract
Reliability is the probability that a system or a product fulfills its intended function without failure over a period of time and it is generally used to determine the reliability, release and testing stop time of the system. The primary objective of this study is to predict and forecast COVID19 reliabilities of the countries by utilizing this definition of the reliability. To our knowledge, this study is the first carried out in the direction of this objective. The major contribution of this study is to model the COVID19 data by considering the intensity functions with different types of functional shapes, including geometric, exponential, Weibull, gamma and identifying best fit (BF) model for each country, separately. To achieve the objective determined, cumulative number of confirmed cases are modelled by eight Non-Homogenous Poisson Process (NHPP) models. BF models are selected based on three comparison criteria, including Root Mean Square Error (RMSE), Normalized Root Mean Square Error (NRMSE), and Theil Statistics (TS). The results can be summarized as follows: S-shaped models provide better fit for 56 of 70 countries. Current outbreak may continue in 43 countries and a new outbreak may occur in 27 countries. 50 countries have the reliability smaller than 75%, 9 countries between 75% and 90%, and 11 countries a 90% or higher on 11 August 2021.

Keywords COVID19 · Reliability · Counting process · Non-homogenous Poisson process · Forecasting

1 Introductıon

Predicting future behavior of COVID19 is extremely important in terms of its early negative effects that may occur on the economy and health sector. So far, many statistical and machine learning modeling techniques have been used to forecast different kinds of behaviors of COVID19 such as number of confirmed, deaths and

✉ Nevin Guler Dincer
nguler@mu.edu.tr

[1] Faculty of Science, Department of Statistics, University of Muğla Sıtkı Koçman, Muğla, Turkey

Published online: 03 July 2022

recovered cases [1–11]. NHPP models such as Gompertz (G) and Logistic Growth (LG) are also among modeling techniques widely utilized to analyze the dynamics of COVID19 since they can easily deal with the nonlinear structure of the COVID19 and have the ability of forecasting the new outbreaks and the end of the outbreak.

Conde-Gutierrez et al. [12] presented a comparative study between the G model and Artificial Neural Networks (ANN) for predicting the cumulative number of deaths in Mexico. They concluded that these modeling techniques provide the good fit. In [13], daily mortality data collected for three European countries, consisting of Greece, France and Italy have also been assessed by G function methods. Diaz Perez et al. [14] have used the G model to forecast the number of infections and mortality for three countries, Austria, Switzerland and Israel. They compared the performance of the G model and ARIMA model. As a result of the comparisons, they found that the G model is more successful in modeling the mortality, while ARIMA model is good at modeling the number of infections. Berihuete et al. [15] developed a model based on G curve and Bayesian inference to investigate the behavior of COVID19 at the three different stages of the pandemic in the province of Cádiz, located at the South of Spain. First, they evaluated the impact of the first lockdown on the COVID19. The second stage that they considered is the lockdown period and lastly, they tried to detect the beginning of the new wave, which would occur after lockdown period. In [16], G function has been used for analyzing the number of infected cases in the 11 countries (Japan, USA, Russia, Brazil, China, Italy, Indonesia, Spain, South Korea, UK and Sweden). Valle [17] has applied the modeling technique based on G function to the data sets, consisting of the total number of infected and deaths by COVID19 in Brazil and two Brazilian states. In [18], Verhulst and G models have been utilized for predicting the effects of COVID19 in Spain. In the result of the study, they concluded that Verhulst and G model have similar prediction performance, but Verhulst model will be more appropriate in modeling the dynamics of COVID19 since its parameters easily tune.

Some studies have used the LG model to predict and forecast the COVID19 data. Kartono et al. [19] have used the LG model to model the cumulative number of confirmed cases in the five countries, including China, Singapore, Saudi Arabia, the Philippines, and Indonesia. In addition, the peak time and turning points of the epidemic are predicted in this study. Simbawa and Aboushoushah [20] have applied LG and its three modified versions to predict the cumulative number of infected cases in Saudi Arabia. They concluded that LG and its modifications provide similar and considerably good predictions results. Mangla et al. [21] have used four modeling techniques, including exponential, G, LG and ARIMA models to predict the cumulative number of confirmed and deaths cases in India and its some states. They found that the ARIMA model provides a better fit for the behavior of COVID19 in India. Liu [22] has aimed to model the cumulative number of confirmed cases in China, involving the time period between 13/02/2020 and 23/03/2020. For this objective, five growth models consisting of LG, G, Mitcherlich, Monomolecular, Negative Exponential have been used. According to five-fold cross validation, they found that LG gives the best predictions. Zhou et al. [23] have also used the LG model for examining the dynamics of COVID19 such as its timing, rate and peak in China and its 20 provinces before and after the suppression.

Al-Dousari et al. [24]. have also used two NHPP models, i.e., Power Law Process and Linear Intensity Functions to predict the number of COVID19 behavior such as the number of new, death and recovered cases for Kuwait considering the COVID19 data collected from the 24th of February 2020 to the 25th of August 2020. Wang [25] and Gholami and Elahian [26] used the piece-wise version of Crow-AMSAA model that is one of the NHPP models to model the spread of COVID19.

These studies generally focused on modeling the number of confirmed or death cases for the specific regions and generally involved the early stage of the pandemic. In addition to this, limited number of NHPP models have been used in the studies cited above. The major contributions of this study can be summarized as follows:

- In this study, eight NHPP models, each of which has the different properties such as functional shape of intensity function or graphical view, are used for modeling COVID19 spread of 70 countries. Thus, the BF model is selected for each country according to the last period of the COVID19 and three comparison criteria.
- The probabilities of lack of occurrences of COVID 19 cases in selected countries and in different time periods are predicted and forecasted by utilizing Poisson distribution. This approach is called as COVID19 reliability.
- Based on the reliability forecasts, it is tried to determine in which countries a new pandemic could be seen, in which countries the current pandemic would continue, and in which countries the pandemic would end.

The organization of this study is as follows. Section 2 gives brief information on NHPP models, parameter estimation method used and reliability forecasting. Section 3 presents the experimental results. Section 4 concludes the study and presents the future works.

2 Materials and Methods

2.1 Some Definitions of NHPP Models

Definition 1 (Counting Process): *A counting process* is a stochastic process $(M(t), t \geq 0)$ that is non-negative, integer-valued, and non-decreasing for all $t \geq 0$. $M(t)$ is the total number of events that occur by time t, and $M(t, t+h) = M(t+h) - M(t)$ denotes the number of events occurred in the time interval $(t, t+h]$, $h > 0$. Besides, a counting process, in which the number of events occurring in non-overlapping time intervals are independent has *independent increments*. A counting process has *the stationary increments* if distribution of $M(t, t+h)$ only depends on the length of time interval [27].

Definition 2 (Poisson Random Variable): If $M(t)$ denotes the number of events that occur in the specified time interval, it is called as *Poisson random variable*. Poisson random variable has the following probability mass function:

$$P(M(t) = k) = \frac{\mathrm{e}^{-\lambda_t} {\lambda_t}^k}{k!} \tag{1}$$

where λ_t is the parameter of Poisson distribution and denotes the average number of events in the specified time interval. Expected value and variance of $M(t)$ are equal to λ_t.

Definition 3 (Poisson Process): $M(t)$ with intensity function λ_t is *the Poisson process* if it has the following properties:

- $M(0) = 0$
- $M(t)$ is the counting process;
- $M(t)$has the independent increments;
- $M(t, t + h) = M(t + h) - M(t)$ is a Poisson random variable with mean $\lambda = \int_t^{t+h} \lambda(z)\mathrm{d}z$ [28].

Definition 4 (Homogeneous Poisson Process): If the Poisson process $M(t)$ has constant intensity function ($\lambda_t = \lambda$ for all time intervals), it is called as *Homogeneous Poisson Process*.

Definition 5 (Non-Homogeneous Poisson Process): If the Poisson process $M(t)$ has the intensity function varying over time, it is *Non-Homogeneous Poisson Process*. The probability mass function of NHPP is defined as follows:

$$\mathrm{P}(M(t, t + h) = k) = \frac{\left(\int_t^{t+h} \lambda(z)\mathrm{d}z\right)^k}{k!} \mathrm{e}^{-\int_t^{t+h} \lambda(z)\mathrm{d}z} \tag{2}$$

Definition 6 (Mean Value Function): A function $\mu(t)$ defined as below is called as the *mean-value function* [28]:

$$E(M(t)) = \mu(t) = \int_0^t \lambda(z)\mathrm{d}z \tag{3}$$

Definition 7 (Reliability) *Reliability* is the probability that an event that can be called as a failure will not occur in a specified period of time. If T is assumed to denote the time to failure, the probability that a failure occurs in the time interval, $[0, t]$:

$$F(t) = P(0 \leq T \leq t) = \int_0^t f(y)\mathrm{d}y \tag{4}$$

where $f(y)$ denotes the failure density function. In this case, reliability is defined as follows:

$$R(t) = P(T > t) = 1 - F(t) = \int_t^{\infty} f(y)\mathrm{d}y \tag{5}$$

3 Non-Homogenous Poisson Process Models

In this study, the use of well-known NHPP models is proposed to forecast the reliability of the selected countries in terms of COVID19 pandemic since following properties of COVID19 are coherent to NHPP models:

- The total number of cases ($M(t)$) is non-negative, integer-valued, and non-decreasing for all $t>0$. In other words, it is a counting process.
- The total number of cases is equal to zero ($M(0) = 0$) at the beginning of the pandemic in the all countries.
- The total number of cases has the independent increments.
- The intensity function (average number of cases) depends on time since it inherently increases or decreases over time. So, the total number of cases has an unstable increment.

Under the assumption that $M(t, t + h)$ is a Poisson random variable with time dependent parameter $\mu(t)$, NHPP models can be used to model COVID19 behavior of the countries and then to predict and forecast the COVID19 reliability. NHPP models are based on estimating the parameters of mean value function, that denotes the total number of events by time t. In the literature, there are many NHPP models that have different properties and mean value functions. These models have been classified in [29, 30] according to their properties as follows:

- Total number of faults observed at infinite time: *finite* or *infinite.*
- The functional shape of fault intensity expressed according to time: *Exponential, Gamma* or *Weibull*.
- The functional shape of fault intensity expressed according to the expected value of observed fault: *geometric* or *power.*
- The graphical view of the mean-value function*: S-shaped* or *concave.*

NHPP models used in this study and their mean value functions are given in Table 1.

As can be seen in Table 1, while some of NHPP models have a shape of concave, some are S-shaped. Concave models provide a better fit for the data sets in which the number of new confirmed cases decreases over time and become constant after a while. S-Shaped models are more appropriate in modeling data sets in which, the

Table 1 The NHPP models used in this study

Model	Mean value function	Properties
Musa logarithmic (ML) model [32]	$\mu(t) = \theta_1 \ln(1 + \theta_2 t)$	Concave, infinite, geometric
Goel-Okumuto (GO) [33]	$\mu(t) = \theta_1 (1 - e^{-\theta_2 t})$	Concave, finite, exponential
Generalized Goel-Okumoto (GGO) [34]	$\mu(t) = \theta_1 (1 - e^{-\theta_2 t^{\theta_3}})$	Concave, finite, Weibull
Inflection S-shaped (ISS) [35]	$\mu(t) = \theta_1 \left(\frac{1-e^{-\theta_2 t}}{1+\theta_3 e^{-\theta_2 t}} \right)$	S-shaped, finite
Delayed S-shaped (DSS) [36]	$\mu(t) = \theta_1 (1 - (1 + \theta_2 t) e^{-\theta_2})$	S-shaped, finite, gamma
Yamada exponential (YE) [37]	$\mu(t) = \theta_1 (1 - e^{-\theta_3 (1 - e^{-\theta_2 t})})$	Concave
Gompertz (G) [38]	$\mu(t) = \theta_1 (\theta_2)^{(\theta_3)^t}$	S-shaped, Gompertz
Logistic growth (LG) [34, 36]	$\mu(t) = \frac{\theta_1}{1+\theta_3 e^{-\theta_2 t}}$	S-shaped, infinite

number of new confirmed cases increases exponentially in the early pandemic and decreases over time in the later period.

4 Parameter Estimation

In order to estimate the parameter of the mean value functions of NHPP models, three estimation methods are generally used: Maximum Likelihood Estimation (MLE), Least Squares (LS) Method, and Nonlinear Least Squares (NLS) Method. The NLS method is preferred in this study, because it provides a solution for all models used here.

In the NLS method, the general form of the regression models which is adapted for the total number of COVID19 cases is as follows:

$$M(t) = \mu(t) + \boldsymbol{\varepsilon} \tag{6}$$

where $\boldsymbol{\varepsilon}$ is the residual vector whose elements correspond to differences between actual values ($M(t)$) and predictions ($\mu(t)$). In the NLS method, it is tried to estimate the parameters which minimizes the sum of squares of residuals as similar to the LS method. In this case, the objective function to be minimized can be written as below:

$$\boldsymbol{C}(\boldsymbol{M}, \boldsymbol{\theta}) = \sum_{i=1}^{n} \varepsilon^2 = \sum_{i=1}^{n} \left(M\left(t_i\right) - \mu(t_i)\right)^2 \tag{7}$$

where $\theta = [\theta_1, \theta_2 \ldots, \theta_p]$ is the parameter vector to be estimated. To estimate these parameter vectors, one of the ways used is that the objective function is differentiated with respect to each$\theta_i (i = 1, 2, \ldots, p)$ separately and the partial derivatives are set to zero. In this way, p equations are obtained. But, they do not solve directly and require the use of numerical optimization methods for the solution because these equations are not closed form. Most popular methods used for this objective are Gauss–Newton (GN), Gradient Descent (GD), and Levenberg–Marquardt (LM). The common property of these algorithms is that they are based on finding the estimate

of parameters which minimize the objective function given in Eq. (7), iteratively. These algorithms consist of three main steps: (i) selecting the initial values of the parameter vector, (ii) updating of the parameter vector in each iteration, (iii) checking the convergence criteria. LM method which is a linear combination of GN and GD is used in this study. In LM, the updating of the parameters is performed as below [39]:

$$\theta_{k+1} = \theta_k - g^{-1}\nabla \mathrm{C} \tag{8}$$

In the Eq. (8), g and ∇C are as follows:

$$g = J^T J + \alpha I \tag{9}$$

$$\nabla C = J^T \varepsilon \tag{10}$$

where J is a gradient vector of ε with respect to θ, α is LM parameter and I is identity matrix.

In the light of these information, the working principle of LM method can be summarized as Table 2.

5 Reliability Forecasting

COVID19 reliability can be defined as the probability of not encountering COVID19 case at a certain time period. Reliability at the time interval $[t, t+h]$ is predicted in NHPP models by following equations:

$$R(h|t) = \mathrm{P}(M(t, t+h) = 0) = \frac{\left(\int_t^{t+h} \lambda(z)\mathrm{d}z\right)^0}{0!} \mathrm{e}^{-\int_t^{t+h} \lambda(z)\mathrm{d}z} \tag{11}$$

$$R(h|t) = \mathrm{e}^{-\int_t^{t+h} \lambda(z)\mathrm{d}z} = \mathrm{e}^{-(\int_0^{t+h} \lambda(z)\mathrm{d}z - \int_0^t \lambda(z)\mathrm{d}z)} \tag{12}$$

Table 2 LM Algorithm

Step 1: Determining initial values of the parameters (θ), LM parameters ($\alpha, \alpha_{\mathrm{up}}, \alpha_{\mathrm{down}}$), J and ε.
Step 2: Calculating vector J by taking partial derivative ε with respect to each θ
Step 3: The value of g is calculated by using Eq. (9)
Step 4:∇C is calculated using Eq. (10)
Step 5: The new values of the parameters are calculated according to Eq. (8)
Step 6: If C_{new} is small than the old value of C, the new values of θ and α are set as:
$\theta = \theta_{k+1}$
$\alpha = \alpha / \alpha_{\mathrm{down}}$
Otherwise,
$\theta = \theta_k$
$\alpha = \alpha * \alpha_{\mathrm{up}}$
Step 7: If the convergence occurs, the algorithm is terminated. Otherwise, go to Step2

From Eq. (3), the formula of the reliability can be rewritten as below:

$$R(h|t) = \mathrm{e}^{-(\mu(t+h)-\mu(t))} \tag{13}$$

$\mu(t+h)$ corresponds to the predicted value of the mean value function at the time $t+h$.

6 Comparison Criteria

To detect the NHPP model that provides the best fitting, three comparison criteria are used as Root Mean Square Error (RMSE), Normalized Root Mean Square Error (NRMSE), and Theil Statistics (TS). These criteria are calculated as below:

$$\mathrm{RMSE} = \sqrt{\frac{\sum_{i=1}^{n} \left(M\left(t_i\right) - \mu(t_i)\right)^2}{n}} \tag{14}$$

$$\mathrm{NRMSE} = \frac{\mathrm{RMSE}}{\max(M(t)) - \min(M(t))} \tag{15}$$

$$\mathrm{TS} = \sqrt{\frac{\sum_{i=1}^{n} \left(M\left(t_i\right) - \mu(t_i)\right)^2}{\sum_{i=1}^{n} M\left(t_i\right)^2}} \tag{16}$$

As seen from Eqs. (14)–(16), all criteria are based on the difference between actual and predicted values. As values of the criteria get smaller, forecasting performance of the models increases.

7 Results and Discussion

In this study, it is aimed that the reliabilities of the countries in terms of COVID19 are forecasted. To achieve this aim, the total number of COVID19 cases of 70 countries are modelled by eight NHPP models given in Table 1. All data sets are downloaded from the website of https://www.kaggle.com/sudalairajkumar/novel-corona-virus-2019-dataset and the time period under consideration is between 22/01/2020 and 10/08/ 2021. Firstly, all datasets are divided into two disjoint subgroups, 80% of which are training (22/01/2020–20/04/2021) and 20% are test sets (21/04/2021–10/08/2021). Training sets are used to estimate the parameters of mean value functions and test sets are used to select the best fit models according to the three comparison criteria defined in Sect. 2.5.

8 Comparison of NHPP Models

This section includes the results related to performance comparison of NHPP models. Figures 1 and 2 show the values of comparison criteria for all countries.

According to Figs. 1 and 2, the results can be summarized as follows:

8.1 For the Training Sets

GO, ML and YE models have similar prediction performance and they generally provide the worst fit. The common property of these models is that they have the shape of concave. Although the ISS model gives the best prediction results for most of the countries, the bad predictions are also obtained from the ISS model for the countries including Armenia, Germany, Greece, Ireland, Kyrgyzstan, Norway, Saudi Arabia, and Turkey. LG and G model also give the good prediction results. Both LG, ISS, and G are S-shaped models. From these results, it can be said that in most of the countries, the number of new cases has increased dramatically at the beginning of the pandemic and then they have declined.

8.2 For the Test Sets

S-shaped models exhibit better fits in most countries. This means that the number of new cases continues to increase at the beginning of the test period (20/04/2021–10/08/2021). Concave models (ML, GO, YE) give the best forecasting results for the countries of Iceland, New Zealand, Nigeria, and Saudi Arabia. This result show that the number of new cases has begun to decrease before the date of 20/04/2021 in these countries.

Figure 2 and Table 3 show the box-plots and descriptive statistics of the comparison criteria, respectively.

In Fig. 3, the line in the middle of the boxes indicates the median of the comparison criteria and the size of the boxes indicates the variation. According to Fig. 3 and Table 3,

- For training sets, the smallest mean value is obtained from G model, while the smallest median value is obtained from the ISS model. LG model is also successful in modeling of the behavior of COVID19 at the beginning of pandemic since the mean and median values of them are also small. The models which have the highest mean and median values are GGO, ML and YE. ISS is the model with the most performance changes according to data set modelled since it has the highest variation coefficient when compared to the G, ML, and LG having the least changes.
- For test sets, the DSS model provides best forecasts. Bad forecasting results are obtained from the GGO model when looking at the mean values. Bad forecasting results are obtained from LG, G and GO models.

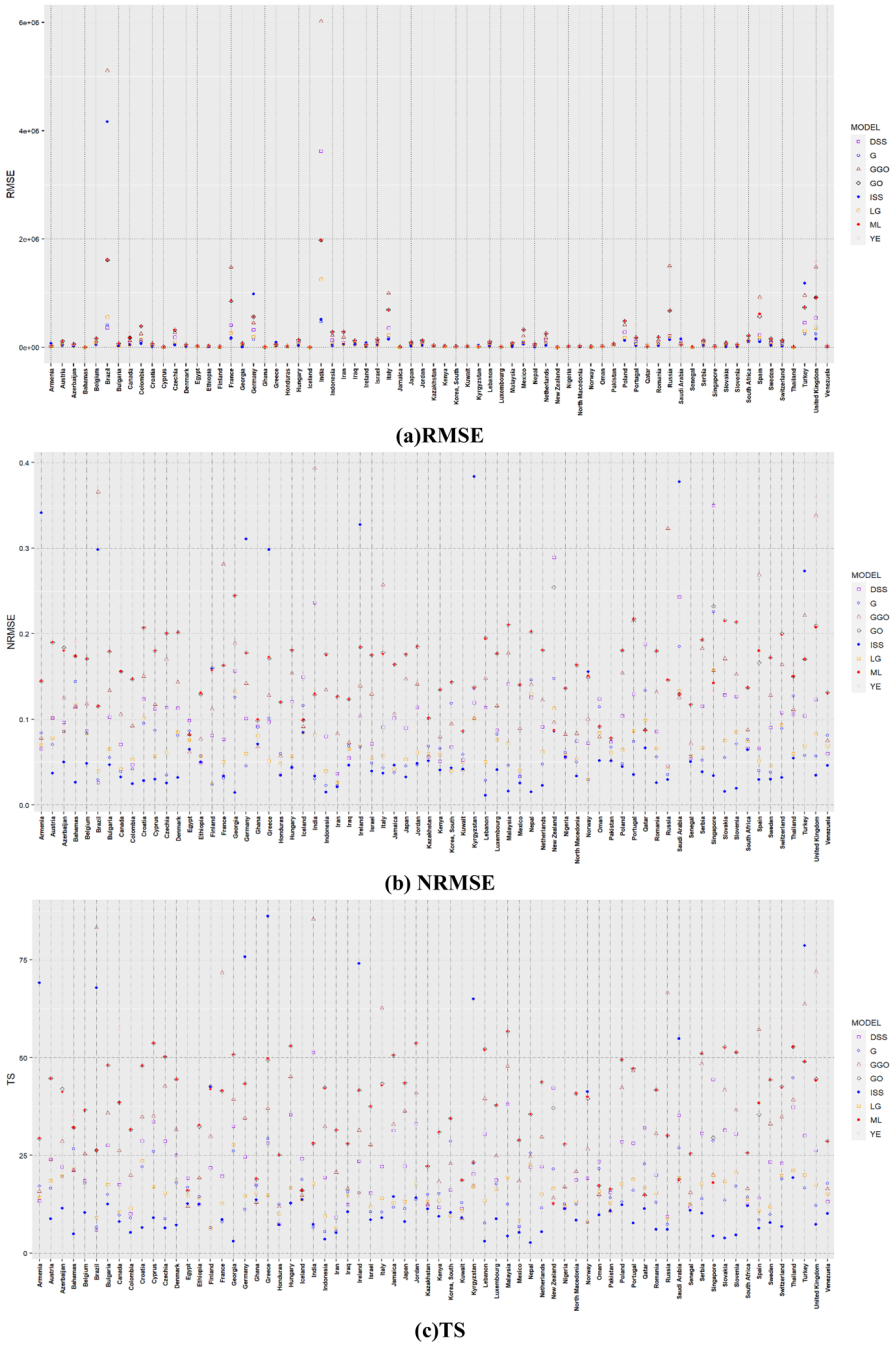

Fig. 1 The values of comparison criteria for the training sets

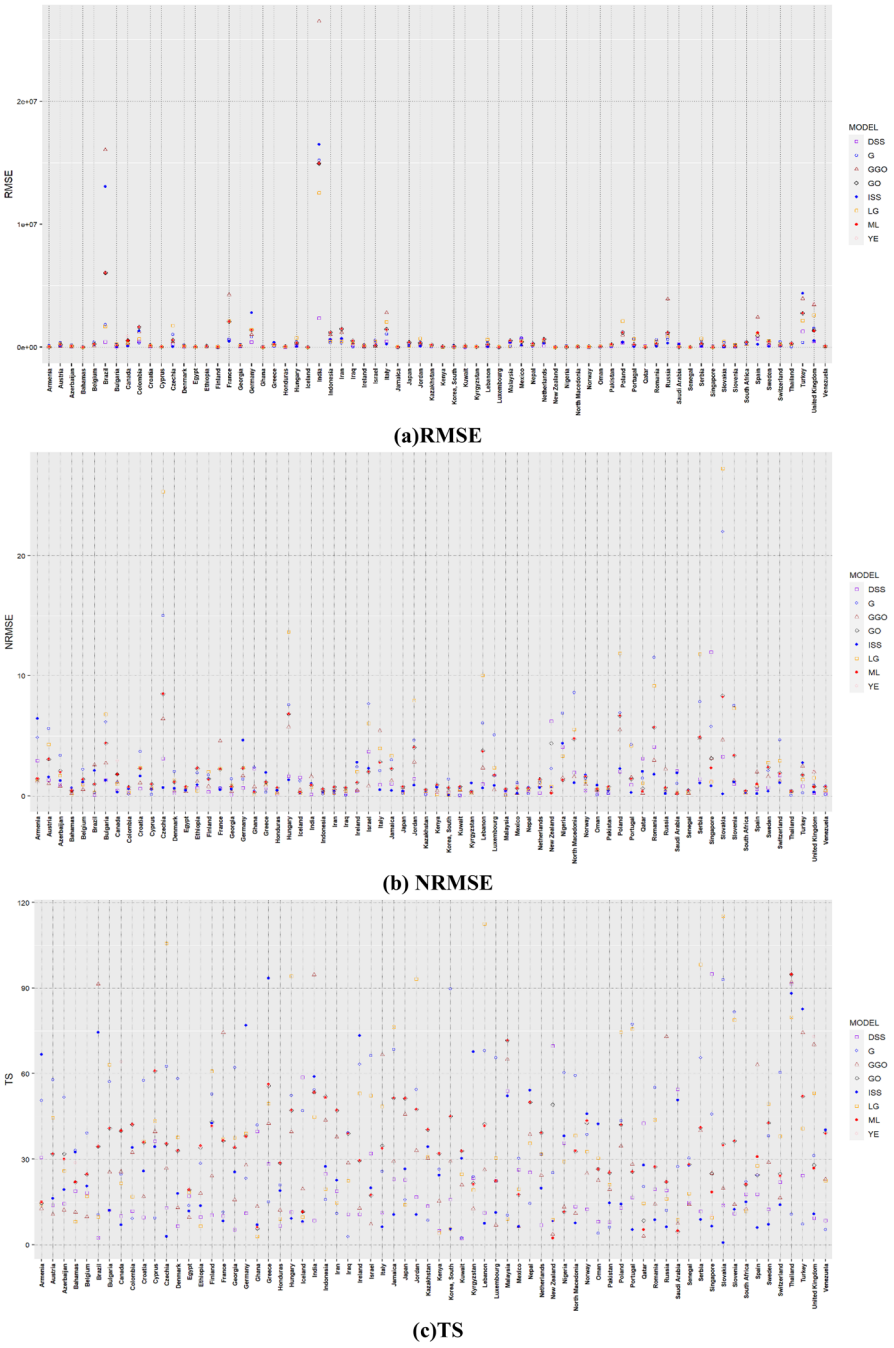

Fig. 2 The values of comparison criteria for the test sets

Table 3 Descriptive statistics of the comparison criteria

	NHPP model	Training			Test		
		RMSE	NRMSE	TS	RMSE	NRMSE	TS
ML	Mean	204,936.48	0.16	36.85	688,317.75	1.85	34.23
	Median	66,790.47	0.17	39.22	184,484.82	1.14	34.28
	Standard deviation	351,508.95	0.04	12.00	1,936,488.52	1.87	15.57
	Variation coefficient	171.52	23.98	32.57	281.34	101.32	45.48
GO	Mean	204,586.70	0.16	37.34	686,501.00	1.92	35.00
	Median	66,763.05	0.17	39.02	185,560.33	1.16	34.57
	Standard deviation	351,009.44	0.04	11.47	1,935,760.45	1.90	15.06
	Variation coefficient	171.57	24.47	30.71	281.97	98.55	43.02
GGO	Mean	330,364.77	0.14	31.76	1,083,422.40	1.45	29.30
	Median	51,373.13	0.12	29.17	105,458.64	0.82	24.23
	Standard deviation	970,491.21	0.07	17.53	3,731,021.50	1.51	22.33
	Variation coefficient	293.76	53.20	55.20	344.37	104.14	76.21
ISS	Mean	131,071.19	0.08	16.87	684,543.97	1.09	26.83
	Median	19,343.86	0.04	9.22	95,069.07	0.71	19.10
	Standard deviation	524,772.12	0.09	20.97	2,530,497.68	1.09	23.20
	Variation coefficient	400.37	126.25	124.31	369.66	100.77	86.49
DSS	Mean	135,327.74	0.10	22.60	218,931.30	1.23	20.75
	Median	47,292.87	0.10	22.10	85,887.50	0.62	14.10
	Standard deviation	438,205.88	0.06	9.51	358,707.75	1.76	18.22
	Variation coefficient	323.81	54.12	42.09	163.84	143.40	87.79
YE	Mean	215,427.07	0.16	37.62	725,488.38	1.88	35.23
	Median	66,765.05	0.17	40.16	184,634.90	1.16	34.51
	Standard deviation	379,860.54	0.05	13.15	1,978,200.59	1.87	16.65
	Variation coefficient	176.33	28.05	34.96	272.67	99.61	47.27
G	Mean	58,640.77	0.07	15.54	530,015.02	2.87	36.94
	Median	27,858.92	0.06	14.25	172,031.99	1.40	31.47
	Standard deviation	85,905.45	0.04	7.07	1,817,691.21	3.84	23.65
	Variation coefficient	146.49	55.80	45.46	342.95	133.66	64.02
LG	Mean	81,009.33	0.07	15.21	612,979.40	2.99	37.25
	Median	28,420.56	0.06	15.13	198,305.49	1.00	30.59
	Standard deviation	170,918.01	0.03	4.16	1,574,655.71	5.09	28.19
	Variation coefficient	210.99	37.36	27.38	256.89	169.85	75.72

9 Best Fit Model Selection

Best fit models to be used in forecasting of reliabilities are selected according to test sets. Table 4 shows the models of the best forecasting results for the countries separately and the values of their comparison criteria.

When looking at the Table 4, it can be seen that

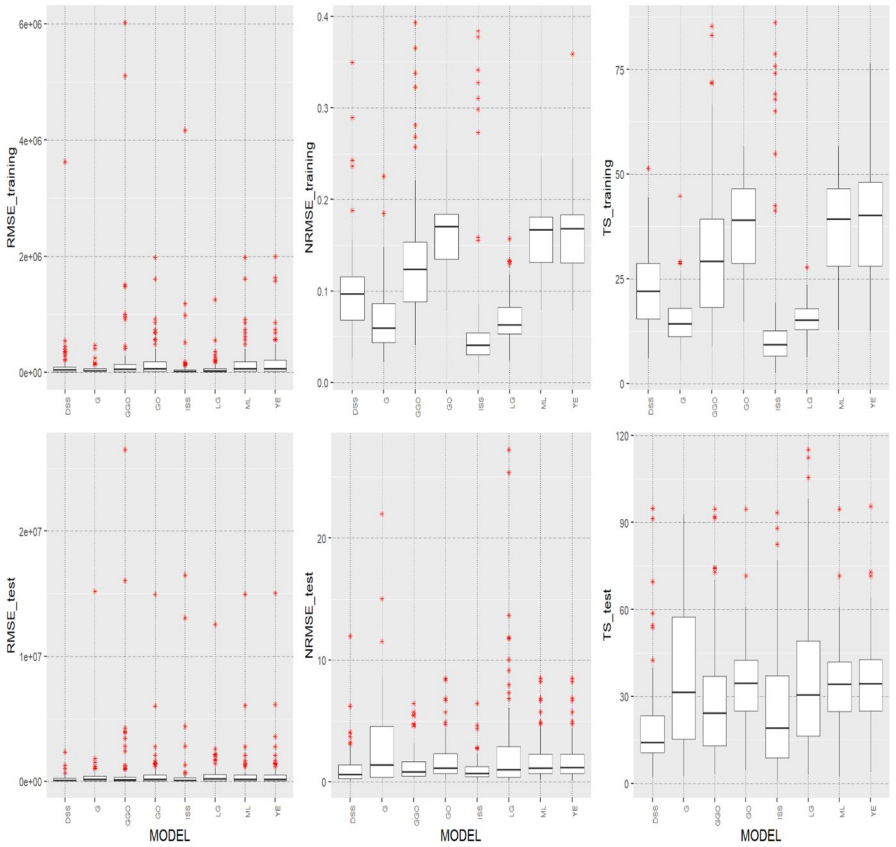

Fig. 3 Box-plots of the comparison criteria according to NHPP models

- The ISS model outperforms for 20 countries, the DSS model for 16 countries, the G model for 13 countries, the GGO model for 10 countries, and the LG model for 7 countries.
- The YE model only becomes successful in forecasting for the countries of Iceland and Saudi Arabia.
- The GO model only outperforms for Nigeria and ML model for New Zealand.
- S-Shaped models are more successful in forecasting the total number of COVID19 cases for 66 of 70 countries. Accordingly, the number of new cases continues to increase in many countries.

10 Reliability Forecasting Results

To forecast the COVID19 reliabilities of the countries, forecast values ($\mu(t)$) normalized as below are used in Eq. (13):

Table 4 Best fit models and values of the comparison criteria

Country	Best fit model	RMSE	NRMSE	TS
Armenia	GGO	28,363.58	1.23	12.69
Austria	GGO	68,774.28	1.03	10.68
Azerbaijan	GGO	40,789.12	0.8	12.23
Bahamas	LG	1001.02	0.16	8.06
Belgium	GGO	104,437.1	0.56	9.78
Brazil	DSS	432,354.2	0.07	2.47
Bulgaria	ISS	50,082.5	1.29	11.99
Canada	ISS	96,779.42	0.32	7.03
Colombia	G	358,718	0.17	9.22
Croatia	DSS	33,920.72	0.62	9.59
Cyprus	G	7389.03	0.15	9.28
Czechia	ISS	47,902.03	0.69	2.89
Denmark	DSS	18,687.06	0.23	6.51
Egypt	GGO	25,419.54	0.38	9.57
Ethiopia	LG	17,540.3	0.44	6.46
Finland	DSS	9898.58	0.34	10.37
France	ISS	478,574	0.51	8.35
Georgia	DSS	18,974.67	0.12	5.25
Germany	DSS	406,159.1	0.67	11.09
Ghana	LG	2870.75	0.17	2.98
Greece	G	62,624.4	0.31	14.97
Honduras	DSS	16,815.1	0.16	6.62
Hungary	ISS	73,669.13	1.33	9.2
Iceland	YE	508.11	0.19	7.41
India	DSS	2,358,272	0.14	8.43
Indonesia	G	367,735	0.17	15.81
Iran	G	345,887.6	0.18	10.96
Iraq	G	36,651.28	0.05	2.78
Ireland	DSS	28,860.33	0.41	10.65
Israel	GGO	61,065.2	0.83	7.2
Italy	ISS	265,767.9	0.52	6.3
Jamaica	ISS	5230.68	0.47	10.6
Japan	LG	108,409.1	0.21	13.96
Jordan	ISS	78,867.83	0.91	10.63
Kazakhstan	G	41,997.18	0.11	8.55
Kenya	LG	7563.04	0.12	4.21
Korea, South	ISS	8571.88	0.09	5.46
Kuwait	DSS	7415.84	0.05	2.2
Kyrgyzstan	GGO	15,642.02	0.2	12.63
Lebanon	ISS	40,636.12	0.67	7.48
Luxembourg	GGO	4835.18	0.53	6.85
Malaysia	LG	68,247.89	0.07	9.14
Mexico	GGO	160,152.9	0.23	6.34

Table 4 (continued)

Country	Best fit model	RMSE	NRMSE	TS
Nepal	G	83,595.53	0.19	14.52
Netherlands	DSS	114,544.6	0.24	6.82
New Zealand	ML	64.31	0.21	2.36
Nigeria	GO	19,378.97	1.32	11.53
North Macedonia	ISS	11,821.28	1.11	7.63
Norway	DSS	15,861.03	0.47	12.47
Oman	G	10,030.47	0.09	4.07
Pakistan	G	57,793.21	0.19	6.16
Poland	DSS	367,604.3	2.04	12.86
Portugal	ISS	46,022.62	0.29	5.21
Qatar	GGO	6597.38	0.22	3.02
Romania	ISS	93,358.72	1.82	8.69
Russia	ISS	338,643.8	0.19	6.31
Saudi Arabia	YE	18,720.32	0.15	3.97
Senegal	DSS	6614.28	0.23	14.14
Serbia	ISS	62,932.21	1.06	8.86
Singapore	ISS	4103.41	0.83	6.56
Slovakia	ISS	2757.49	0.17	0.71
Slovenia	DSS	27,693.5	1.01	10.94
South Africa	LG	226,951.7	0.23	11.71
Spain	ISS	231,026.8	0.19	5.98
Sweden	ISS	75,585.32	0.4	7.12
Switzerland	ISS	97,688.35	1.09	14.07
Thailand	G	34,957.22	0.05	10.74
Turkey	G	387,311	0.24	7.29
United Kingdom	DSS	456,888.9	0.26	9.33
Venezuela	G	13,591.91	0.11	5.32

$$\widetilde{\mu(t)} = \frac{\mu(t)}{\text{population size}} * 10000 \tag{17}$$

The reason for this kind of normalization is to prevent the population sizes of countries from affecting the reliability estimates negatively. Besides, the reliability forecasts are valid for the total number of COVID19 cases per 10,000 persons.

For example, the population size of Turkey is 82 million. If the difference between successive forecast values ($\mu(t+h) - \mu(t)$) is equal to or less than 820, in other words, the number of daily new cases is equal to 820 or less, the reliability of Turkey will be forecasted as 0.90 or more. To achieve reliability of 0.999 or more, the number of daily new cases must be equal to 8 or less. These results are only valid for Turkey since the calculations are based on the population size. To achieve these reliability forecasts, the number of daily new cases should be smaller in countries with a small population size and larger in countries with a

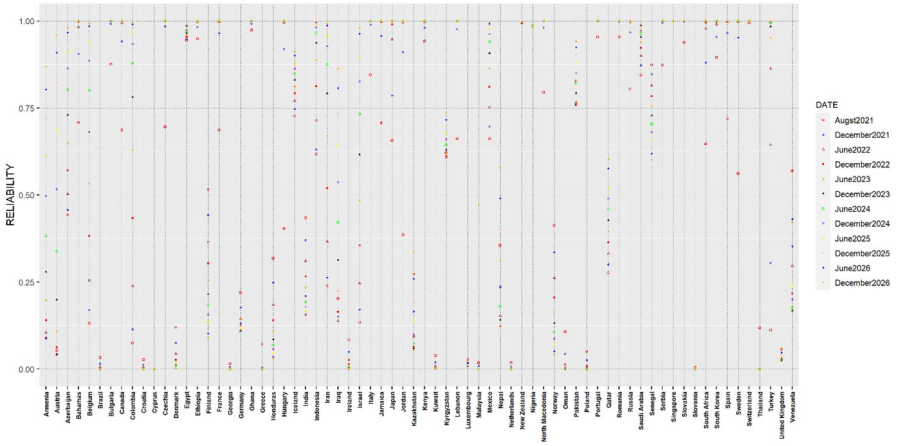

Fig. 4 Reliability forecasts

large population size. Figure 4 shows the reliability values forecasted for twelve different time points.

As can be seen Fig. 4,

- The top 5 countries with the highest reliability are Singapore, New Zealand, Switzerland, Nigeria and Ghana by the date of August 11, 2021.
- The five countries having the least reliability are Cyprus, Slovenia, Georgia, Malaysia and Netherlands on the date of August 11, 2021.
- The countries, which have the reliability of 90% and more by the date of August 11, 2021 are Egypt, Ethiopia, Ghana, Kenya, New Zealand, Nigeria, Portugal, Romania, Singapore, Slovakia, and Switzerland.
- The countries whose reliabilities decrease over time are Brazil, Croatia, Cyprus, Denmark, Finland, Georgia, Germany, Greece, Honduras, India, Ireland, Kuwait, Luxembourg, Netherlands, Norway, Oman, Poland, Slovenia, Thailand, United Kingdom and Venezuela. This result can be interpreted that new outbreak can occur in these countries.
- In Bahamas, Bulgaria, Canada, Czechia, Egypt, Ethiopia, France, Ghana, Hungary, Italy, Jamaica, Jordan, Kenya, Lebanon, New Zealand, Nigeria, North Macedonia, Portugal, Romania, Russia, Serbia, Singapore, Slovakia, South Korea, Spain, Sweden and Switzerland, the current outbreak can end until the end of 2021 because their reliabilities are higher than 90% in this date.
- Azerbaijan, Belgium, Colombia, Iceland, Indonesia, Iran, Israel, Japan, Kyrgyzstan, Mexico, Qatar, South Africa, Turkey and Saudi Arabia are also among the countries where the current outbreak will continue.
- The reliability of Colombia, Iran, Indonesia and Turkey will increase significantly until the end of 2023. It is forecasted that the reliabilities of Columbia, Iran, Indonesia, and Turkey will be 0.78, 0.79, 0.94 and 0.98, respectively at the end of 2023.

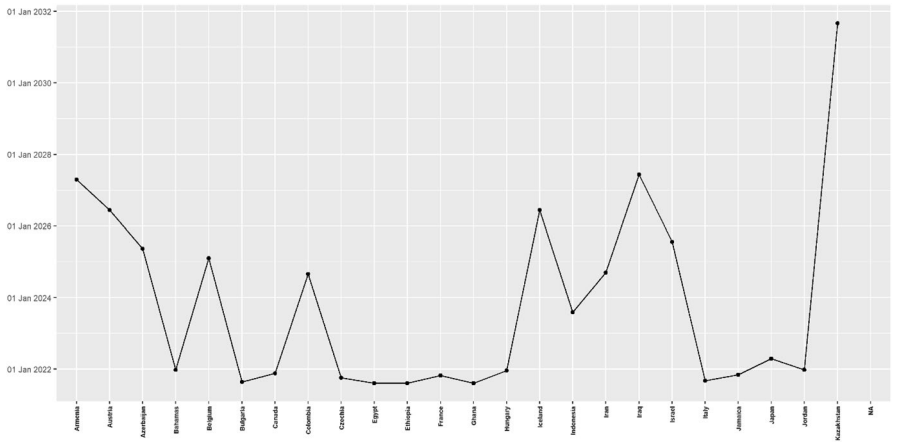

Fig. 5 The dates that reliabilities reach to above 90%

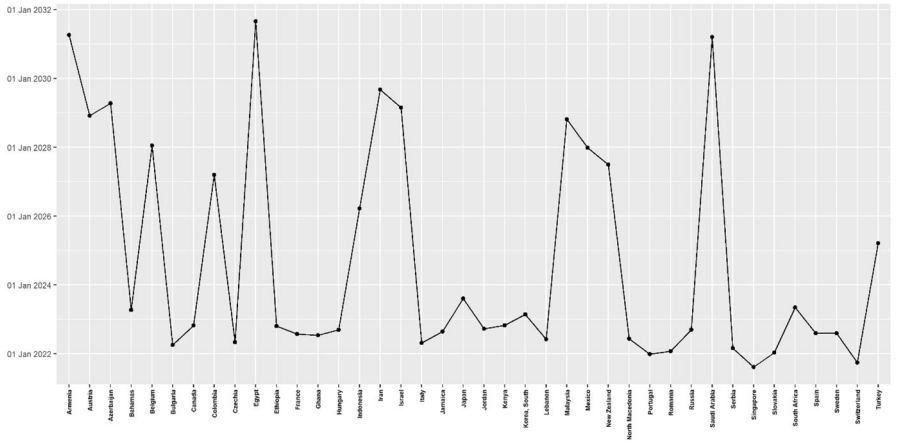

Fig. 6 The dates that reliabilities reach to above 99.9%

Figures 5, 6, and Table 5 show the dates which the reliabilities reach to above 90% and 99.9%.

As can be seen from Figs. 5, 6, and Table 5,

- The reliabilities of 11 countries are equal or higher than 90% on the date of 11 August, 2021. These countries are Egypt, Ethiopia, Ghana, Kenya, New Zealand, Nigeria, Portugal, Romania, Singapore, Slovakia, and Switzerland. The reliability of Singapore is equal or higher than 99.9%.
- Countries whose reliabilities reach 90% until the end of 2021 are Bahamas, Bulgaria, Canada, Czechia, France, Hungary, Italy, Jamaica, Jordan, Lebanon, North Macedonia, Russia, Serbia, South Korea, Spain, and Sweden.

Table 5 The Dates of Reliability ≥ 90% and ≥ 99.9%

Country	> 0.90	> 0.999	Country	> 0.90	> 0.999
Armenia	19-Apr-2027	07-Apr-2031	Kenya	11-Aug-2021	28-Oct-2022
Austria	13-Jun-2026	30-Nov-2028	Kuwait	> 29-Sep-2033	> 29-Sep-2033
Azerbaijan	14-May-2025	13-Apr-2029	Kyrgyzstan	22-Dec-2031	> 29-Sep-2033
Bahamas	24-Dec-2021	10-Apr-2023	Lebanon	19-Oct-2021	03-Jun-2022
Belgium	07-Feb-2025	21-Jan-2028	Luxembourg	> 29-Sep-2033	> 29-Sep-2033
Brazil	> 29-Sep-2033	> 29-Sep-2033	Malaysia	16-Jul-2027	24-Oct-2028
Bulgaria	23-Aug-2021	05-Apr-2022	Mexico	24-Nov-2023	26-Dec-2027
Canada	20-Nov-2021	26-Oct-2022	Nepal	14-Nov-2029	> 29-Sep-2033
Colombia	29-Aug-2024	15-Mar-2028	Netherlands	> 29-Sep-2033	> 29-Sep-2033
Croatia	> 29-Sep-2033	> 29-Sep-2033	New Zealand	11-Aug-2021	30-Jun-2027
Cyprus	> 29-Sep-2033	> 29-Sep-2033	Nigeria	11-Aug-2021	> 29-Sep-2033
Czechia	06-Oct-2021	03-May-2022	North Macedonia	25-Sep-2021	10-Jun-2022
Denmark	> 29-Sep-2033	> 29-Sep-2033	Norway	> 29-Sep-2033	> 29-Sep-2033
Egypt	11-Aug-2021	30-Aug-2031	Oman	> 29-Sep-2033	> 29-Sep-2033
Ethiopia	11-Aug-2021	22-Oct-2022	Pakistan	02-Dec-2025	> 29-Sep-2033
Finland	> 29-Sep-2033	> 29-Sep-2033	Poland	> 29-Sep-2033	> 29-Sep-2033
France	28-Oct-2021	29-Jul-2022	Portugal	11-Aug-2021	27-Dec-2021
Georgia	> 29-Sep-2033	> 29-Sep-2033	Qatar	> 29-Sep-2033	> 29-Sep-2033
Germany	> 29-Sep-2033	> 29-Sep-2033	Romania	11-Aug-2021	27-Jan-2022
Ghana	11-Aug-2021	17-Jul-2022	Russia	06-Oct-2021	11-Sep-2022
Greece	> 29-Sep-2033	> 29-Sep-2033	Saudi Arabia	26-Jun-2022	16-Mar-2031
Honduras	> 29-Sep-2033	> 29-Sep-2033	Senegal	> 29-Sep-2033	> 29-Sep-2033
Hungary	18-Dec-2021	11-Sep-2022	Serbia	21-Aug-2021	28-Feb-2022
Iceland	11-Jun-2026	> 29-Sep-2033	Singapore	11-Aug-2021	11-Aug-2021
India	> 29-Sep-2033	> 29-Sep-2033	Slovakia	11-Aug-2021	13-Jan-2022
Indonesia	05-Aug-2023	22-Mar-2027	Slovenia	> 29-Sep-2033	> 29-Sep-2033
Iran	13-Sep-2024	05-Sep-2028	South Africa	20-Jan-2022	06-May-2023
Iraq	10-Jun-2027	22-Jun-2033	South Korea	21-Aug-2021	23-Feb-2023
Ireland	> 29-Sep-2033	> 29-Sep-2033	Spain	23-Oct-2021	05-Aug-2022
Israel	26-Jul-2025	26-Feb-2029	Sweden	18-Nov-2021	07-Aug-2022
Italy	05-Sep-2021	25-Apr-2022	Switzerland	11-Aug-2021	30-Sep-2021
Jamaica	04-Nov-2021	25-Aug-2022	Thailand	> 29-Sep-2033	> 29-Sep-2033
Japan	17-Apr-2022	09-Aug-2023	Turkey	24-Feb-2023	20-Mar-2025
Jordan	24-Dec-2021	22-Sep-2022	United Kingdom	> 29-Sep-2033	> 29-Sep-2033
Kazakhstan	03-Sep-2031	> 29-Sep-2033	Venezuela	22-Jul-2031	> 29-Sep-2033

- Countries whose reliabilities reach 99.9% until the end of 2021 are Portugal and Switzerland.
- Countries whose reliabilities reach 90% until the end of 2022 are Japan, Saudi Arabia, and South Africa.

- Countries whose reliabilities reach 99.9% until the end of 2022 are Bulgaria, Canada, Czechia, Ethiopia, France, Ghana, Hungary, Italy, Jamaica, Jordan, Kenya, Lebanon, North Macedonia, Romania, Russia, Serbia, Slovakia, Spain and Sweden.
- Indonesia, Mexico and Turkey will have the 90% or higher reliabilities and Japan, South Korea, Bahamas and South Africa will have the 99.9% or higher reliabilities until the end of 2023.
- Armenia, Austria, Azerbaijan, Belgium, Colombia, Iceland, Iran, Iraq, Israel, Kazakhstan, Kyrgyzstan, Malaysia, Nepal, Pakistan, Venezuela will reach a level of 90% reliability after the date of 2023.

11 Conclusions and Future Works

11.1 Conclusion

In this study, the COVID19 reliabilities of 70 countries are forecasted by using eight NHPP models which have different intensity functions and graphical views. To achieve this objective, a procedure, consisting of three main steps, is followed. The first step includes estimating the parameters of mean-value functions of NHPP models by using the LM algorithm. In this step, the parameters of 560 (70*8) NHPP models are estimated. In the second step, the BF model is selected according to the three comparison criteria and the test sets for each country. In the last step, COVID19 reliabilities are forecasted by using the NHPP model selected as BF. The results can be summarized as follows:

- S-shaped models provide the best fitting for 56 of 70 countries.
- On 11 August 2021,

    o 50 countries have the reliability smaller than 75%. These countries are Armenia, Austria, Azerbaijan, Bahamas, Belgium, Brazil, Canada, Colombia, Croatia, Cyprus, Czechia, Denmark, Finland, France, Georgia, Germany, Greece, Honduras, Hungary, Iceland, India, Indonesia, Iran, Iraq, Ireland, Israel, Jamaica, Japan, Jordan, Kazakhstan, Kuwait, Kyrgyzstan, Lebanon, Luxembourg, Malaysia, Mexico, Nepal, Netherlands, Norway, Oman, Poland, Qatar, Slovenia, South Africa, Spain, Sweden, Thailand, Turkey, United Kingdom, and Venezuela.

    p The reliabilities between 0.75 and 0.9 are obtained for 9 countries, including Bulgaria, Italy, North Macedonia, Pakistan, Russia, Saudi Arabia, Senegal, Serbia, and South Korea.

    q Egypt, Ethiopia, Ghana, Kenya, New Zealand, Nigeria, Portugal, Romania, Singapore, Slovakia, and Switzerland have the reliabilities higher than 90%.

- Countries whose reliability is expected to exceed 0.90 by the end of 2022 are Bahamas, Canada, Czechia, France, Hungary, Italy, Jamaica, Japan, Jordan,

Lebanon, North Macedonia, Russia, Saudi Arabia, Serbia, South Africa, South Korea, Spain, and Sweden.

- Countries whose reliability is expected to exceed 0.90 by the end of 2023 are Indonesia, Mexico, and Turkey.
- At the end of 2024, Colombia and Iran are expected to have reliabilities with 0.935 and 0.928, respectively.
- In 27 countries, new outbreaks can occur since their reliabilities decrease over time. These countries are Brazil, Croatia, Cyprus, Denmark, Finland, Georgia, Germany, Greece, Honduras, India, Iraq, Ireland, Kazakhstan, Kuwait, Luxembourg, Malaysia, Nepal, Netherlands, Norway, Oman, Pakistan, Poland, Senegal, Slovenia, Thailand, United Kingdom and Venezuela. Countries whose reliability is expected to increase in 2023 among these countries are Iraq, Kazakhstan, Nepal, Pakistan, and the United Kingdom.
- Current outbreak is expected to continue in 43 countries, including Armenia, Austria, Azerbaijan, Bahamas, Belgium, Bulgaria, Canada, Colombia, Czechia, Egypt, Ethiopia, France, Ghana, Hungary, Iceland, Indonesia, Iran, Israel, Italy, Jamaica, Japan, Jordan, Kenya, Kyrgyzstan, Lebanon, Mexico, New Zealand, Nigeria, North Macedonia, Portugal, Qatar, Romania, Russia, Saudi Arabia, Serbia, Singapore, Slovakia, South Africa, South Korea, Spain, Sweden, Switzerland, and Turkey.
- Countries that are expected to have the mean reliability above 50% in 2022 are Azerbaijan, Bahamas, Bulgaria, Canada, Czechia, Egypt, Ethiopia, France, Ghana, Hungary, Iceland, Indonesia, Italy, Jamaica, Japan, Jordan, Kenya, Kyrgyzstan, Lebanon, Mexico, New Zealand, Nigeria, North Macedonia, Pakistan, Portugal, Romania, Russia, Saudi Arabia, Senegal, Serbia, Singapore, Slovakia, South Africa, South Korea, Span, Switzerland, and Turkey.
- Countries where the reliability is expected to be low by 2033 are Brazil, Croatia, Cyprus, Denmark, Finland, Georgia, Germany, Greece, Honduras, India, Ireland, Kuwait, Luxembourg, Netherlands, Norway, Oman, Poland, Qatar, Senegal, Slovenia, Thailand, and the United Kingdom.

11.2 Future Works

We can summarize our future works as follows:

- In this study, the reliabilities have been forecasted by considering the cumulative number of confirmed cases. We are planning to forecast the reliabilities by considering the cumulative number of deaths, recovered and confirmed cases simultaneously.
- NHPP models developed in the last years and popular machine learning modeling techniques are planned to be used for forecasting the reliability. The probability distributions of the predicted values obtained from the machine learning modeling techniques will be used to find the reliability forecasts.
- We are planning to cluster countries according to the COVID19 reliabilities from period to period.

- Fuzzy reliability models are planned to be developed.

Supplementary Information The online version contains supplementary material available at https://doi.org/10.1007/s00354-022-00183-1.

Declarations

Conflict of Interest The authors have no conflicts of interest to declare that are relevant to the content of this article.

References

1. Hernandez-Matamoros, A., Fujita, H., Hayashi, T., Perez-Meana, H.: Forecasting of COVID19 per regions using ARIMA models and polynomial function. Appl. Soft Comput. **96**, 106610 (2020)
2. Roy, S., Bhunia, G.S., Shit, P.K.: Spatial prediction of COVID19 epidemic using ARIMA techniques in India. Model. Earth Syst. Environ. **7**, 1385–1391 (2020)
3. Malki, Z., Atlam, E., Ewis Dagnew, A.G., Alzighaibi, A.R., Elmarhomy, G., Elhosseini, M.A., Hassanien, A.E., Gad, I.: ARIMA models for predicting the end of COVID19 pandemic and the risk of second rebound. Neural Comput. Appl. **33**, 2929–2948 (2021)
4. Perone, G.: Comparison of ARIMA, ETS, NNAR, TBATS and hybrid models to forecast the second wave of COVID19 hospitalizations in Italy. Eur. J. Health Econ. https://link.springer.com/article/10.1007%2Fs10198-021-01347-4 (2021)
5. Pinter, G., Felde, I., Mosavi, A., Ghamisi, P., Gloaguen, R.: COVID19 Pandemic prediction for Hungary: a hybrid machine learning approach. Mathematics **8**(6), 1–20 (2020)
6. Ardabili, S.F., Mosavi, A., Ghamisi, P., Ferdinand, F., Varkonyi-Koczy, A.R., Reuter, U., Rabczuk, T., Atkinson, P.M.: COVID19 outbreak prediction with machine learning. Algorithms **13**(10), 1–36 (2020)
7. Singh, V., Poonia, R.C., Kumar, S., Dass, P., Agarwal, P., Bhatnagar, V., Raja, L.: Prediction of COVID19 coronavirus pandemic based on time series data using support vector machines. J. Discr. Math. Sci. Cryptogr. **23**(8), 1584–1597 (2020)
8. Muhammad, L.J., Algehyne, E.A., Usman, S.S., Ahmad, A., Chakraborty, C., Mohammed, I.A.: Supervised machine learning models for prediction of COVID19 infection using epidemiology dataset. SN Comp. Sci. **11**, 2–11 (2021)
9. Abbasimehr, H., Paki, R.: Prediction of COVID19 confirmed cases combining deep learning methods and Bayesian Optimization. Chaos Solit. Fract. **142**(110511), 1–14 (2021)
10. Kim, M.: Prediction of COVID19 confirmed cases after vaccination: based on statistical and deep learning models. Sci. Med. J. **3**(2), 153–165 (2021)
11. Toğa, G., Atalay, B., Toksarı, M.D.: COVID19 prevalence forecasting using autoregressive integrated moving average (ARIMA) and artificial neural networks (ANN): case of Turkey. J. Inflect. Public Health. **14**(7), 811–816 (2021)
12. Conde-Gutierrez, R.A., Colorado, D., Hernandez-Bautista, S.L.: Comparison of an artificial neural networks and Gompertz model for predicting the dynamics of deaths from COVID19 in Mexico. Nonlinear Dyn. **104**, 4655–4669 (2021)
13. Spanakis, M., Zoumpoulakis, M., Patelarou, A.E., Patelarou, E., Tzanakis, N.: COVID19 epidemic: comparison of three European countries with different outcome using Gompertz function method. Pneumonia **33**(2), 1–6 (2020)
14. Diaz Perez, F.J., Chinarro, D., Otin, R.P., Diaz Martin, R., Diaz, M., Mouhaffel, G.: Comparison of growth patterns of COVID19 cases through the ARIMA and Gompertz models case studies, Austria, Switzerland and Israel. Rambam Maimonides Med. J. **11**(3), e0022 (2020)
15. Berihuete, A., Sanchez-Sanchez, M., Suarez-Llorens, A.: A Bayesian model of COVID19 cases based on Gompertz Curve. Mathematics **9**(228), 1–16 (2021)
16. Ohnishi, A., Namekawa, Y., Fukui, T.: Universality in COVID19 spread in the view of the Gompertz function. Progr. Theor. Exp. Phys. **12**, 123J01 (2020). https://doi.org/10.1093/ptep/ptaa148

17. Valle, J.A.M.: Predicting the number of total COVID19 cases and deaths in Brazil by the Gompertz model. Nonlinear Dyn. **102**, 2951–2957 (2020)
18. Fernandez-Martinez, J.L., Fernandez-Muniz, Z., Cernea, A., Kloczkowski, A.: Predictive mathematical models of the Short-Term and Long-Term growth of the COVID19. Comput. Math. Methods Med. **2021**, 1–14 (2021)
19. Kartono, A., Wahyudi, S.T., Setiawan, A.A., Sofian, I.: Predicting of the Coronavirus disease 2019 (COVID19) epidemic using estimation of the parameters in the logistic growth models. Infect. Dis. Rep. **13**, 465–485 (2021)
20. Simbawa, E., Aboushoushah, S.: Logistic growth model and modified versions for the cumulative number of confirmed cases of COVID19 in Saudi Arabia. Commun. Math. Biol. Neurosci. **19** (2021)
21. Mangla, S., Pathak, A.K., Arshad, M., Haque, U.: Short-term forecasting of the COVID19 outbreak in India. Int. Health (2021). https://doi.org/10.1093/inthealth/ihab031
22. Liu, Z.: Uncertain growth model for the cumulative number of COVID19 infections in China. Fuzzy Optim. Decis. Making **20**, 229–242 (2021)
23. Zou, Y., Pan, S., Zhao, P., Han, L., Wang, X., Hemerik, L., Knops, J., Van der Werf, W.: Outbreak analysis with a logistic growth model shows COVID19 suppression dynamics in China. Plos One **15**(6), e0235247 (2020)
24. Al-Dousari, A., Ellahi, A., Hussain, I.: Use of non-homogenous Poisson process for the analysis of new cases, death, and recoveries of COVID-19 patients: a case study of Kuwait. J. King Saud Univ. Sci. **33**(8), 101614 (2021)
25. Wang, Y.: Predict new cases of the coronavirus 19; in Michigan U.S.A. or other countries using Crow-AMSAA method. Inf. Dis. Model. **5**, 459–477 (2020)
26. Gholami, P., Elahian, S.: Use piecewise Crow-AMSAA method to predict infection and death of coronavirus in Iran. Int. J. Reliab. Risk Saf. Theory Appl. **3**(2), 71–80 (2020)
27. Bas, E.: A brief introduction to point process, counting process, renewal process, regenerative process, Poisson process. In: Basics of probability and stochastic processes. Springer (2019)
28. Daniel, J.W.: Poisson process (and mixture distributions). Jim Daniel's Actuarial Seminars. http://www.actuarialseminars.com/ (2019)
29. Musa, J.D., Okumoto, K.: Software reliability models: concepts, classification, comparisons, and practice. In: Skwirzynski, J.K. (ed.) Electronic Systems Effectiveness and Life Cycle Costing. NATO ASI Series (Series F: Computer and Systems Sciences), vol. 3. Springer, Berlin, Heidelberg (1983)
30. Belli, F., Beyazıt, M., Güler Dincer, N.: Event-oriented, model-based GUI testing and reliability assessment—approach and case study. Adv. Comp. **85**, 279–326 (2012)
31. Vizarreta, P., Trivedi, K., Helvik, B., Heegaard, P., Blenk, A., Kellerer, W., Machuca, C.M.: Assessing the maturity of SDN controllers with software reliability growth models. IEEE Trans. Netw. Serv. Manage. **15**(3), 1090–1104 (2018)
32. Musa, J.D., Okumoto, K.: A logarithmic Poisson execution time model for software reliability measurement. In: Proc. 7th International Conference Software Engineering, pp. 230–238 (1984)
33. Goel, A.L., Okumoto, K.: A time dependent error detection rate model for software reliability and other performance measures. IEEE Trans. Reliab. **R-28**, 206–211 (1979)
34. Lyu, M.R.: Handbook of Software Reliability Engineering. IEEE Comput. Soc. Press, Los Alamitos, CA, USA (1996)
35. Ohba, M.: Software reliability analysis models. IBM J. Res. Dev. **28**(4), 428–443 (1984)
36. Yamada, S., Ohba, M., Osaki, S.: S-shaped reliability growth modeling for software error detection. IEEE Trans. Reliab. **R-32**(5), 475–484 (1983)
37. Yamada, S., Ohtera, H., Narihisa, H.: Software reliability growth models with testing-effort. IEEE Trans. Reliab. **35**(1), 19–23 (1986)
38. Ohishi, K., Okamura, H., Dohi, T.: Gompertz software reliability model: estimation algorithm and empirical validation. J. Syst. Softw. **82**(3), 535–543 (2009)
39. Transtrum, M.K., Macha, B.B., Sethna, J.P.: Geometry of nonlinear least squares with applications to sloppy models and optimization. Phys. Rev. E **83**, 036701 (2011)